AIAA JOURNAL
Vol. 43, No. 9, September 2005

# Technical Notes

*TECHNICAL NOTES are short manuscripts describing new developments or important results of a preliminary nature. These Notes should not exceed 2500 words (where a figure or table counts as 200 words). Following informal review by the Editors, they may be published within a few months of the date of receipt. Style requirements are the same as for regular contributions (see inside back cover).*

## Feedback Linearization Control for Panel Flutter Suppression with Piezoelectric Actuators

Seong Hwan Moon*
*Korea University of Technology and Education, Chungnam 330-708, Republic of Korea*
Dongkyoung Chwa†
*Ajou University, Suwon 443-749, Republic of Korea*
and
Seung Jo Kim‡
*Seoul National University, Seoul 151-742, Republic of Korea*

### I. Introduction

PANEL flutter is a self-excited dynamic instability phenomenon under the supersonic/hypersonic environment. It is caused and maintained by the interactions between motions of an aircraft structural panel and aerodynamic loads exerted on one side of the panel.

Many studies on panel flutter have been carried out for many years. Gray and Mei[1] gave an excellent survey on various theoretical considerations for the investigation of nonlinear panel flutter up to 1991. Mei et al.[2] presented an extensive review of the developments and advances in nonlinear panel flutter analysis and experiment up to 1999. Zhou et al.[3] presented a finite element time-domain modal approach for the analysis of nonlinear flutter of composite panels at elevated temperatures. The piezoelectric material has been used in the field of works on panel flutter suppression by active or passive control scheme.

Scott and Weisshaar[4] investigated the feasibility of piezoelectric actuator for linear panel flutter for the first time. Zhou et al.[5] extended this study to the nonlinear panel flutter problems. Frampton et al.[6] investigated an active control of linear panel flutter by using a collocated direct rate feedback controller. In contrast to the active control, Suleman and Goncalves[7] investigated the feasibility of passive control methodology for linear panel flutter suppression using piezoelectric patches. Moon and Kim[8] presented a comparison between active control scheme and passive suppression scheme by using finite element method. They used a lead zirconate titanate (PZT) actuator connected with an inductor-resistor series shunt circuit for passive suppression system. Moon and Kim[9] also developed an active/passive hybrid control scheme for the nonlinear panel flutter suppression by using piezoelectric actuators connected in series with an external voltage source and a passive resonant shunt circuit.

However, in the previous studies on panel flutter suppression using piezoelectric materials, an optimal controller has been designed based on the linear model. In general, there exists a maximum suppressible dynamic pressure $\lambda_{max}$ under which the flutter motions can be completely suppressed.[5] That is, the flutter motions can no longer be suppressed beyond $\lambda_{max}$ because of the limitation of the maximum electric field of piezoelectric actuators. When the optimal controller based on the linear model is applied for the actual nonlinear system, a relatively low $\lambda_{max}$ is expected.

The system to be controlled in this Note is both nonlinear and underactuated (i.e., systems with a fewer number of independent actuators than degrees of freedom). Because the nonlinear system can be better controlled by the nonlinear control method, there have been many studies on nonlinear control method (in particular, feedback linearization control[10]) for many systems, for example, robotics,[11] missiles,[12] motors,[13] etc. Also, there has been much interest in the control of underactuated mechanical systems[14] such as two-wheeled mobile robot,[15] underactuated rigid spacecrafts,[16] and underactuated ships.[17]

In this study, to consider the nonlinear characteristics of the model equations and also obtain the higher $\lambda_{max}$ with a lower control input, a nonlinear controller using feedback linearization method is proposed. Feedback linearization, one of the commonly used geometric nonlinear control techniques, is a powerful technique that takes the nonlinearities into account directly. Unlike the previous linear quadratic regulator (LQR) controller based on the linear model, the nonlinear controller is designed based on the nonlinear model. Because the control gain is determined based on the nonlinear coupled-modal model, the range of the maximum suppressible dynamic pressure $\lambda_{max}$ can be enlarged, compared with the LQR controller based on the linear model. Because the system to be controlled is also underactuated, only partial linearization is possible (one state among six states can be linearized). Instead of using partial feedback linearization as in Ref. 18, we use the pseudoinverse instead of inverse in the control input caused by the underactuation. In Ref. 18, partial feedback linearization and LQR methods are combined for the vibration suppression of the flexible beam.

### II. Governing Equation

**Variational Formulation**

For a piezolaminated composite panel, the mechanical response and the electrical response are governed by the stress-equilibrium equation and Maxwell's equation, respectively,

$$\nabla \cdot \boldsymbol{\sigma} + \boldsymbol{f}_b = \rho \ddot{\boldsymbol{u}} \tag{1}$$

$$\nabla \cdot \boldsymbol{D} = 0 \tag{2}$$

where $\boldsymbol{\sigma}$ is the stress, $\boldsymbol{f}_b$ is the body force, $\rho$ denotes material density for a given layer, $\boldsymbol{u}$ is displacement, and $\boldsymbol{D}$ is electric displacement.

By using the variational principle and the divergence theorem, one can derive equivalent variational form as

$$\int_V \rho(\delta\boldsymbol{u})^T \ddot{\boldsymbol{u}}\,\mathrm{d}V + \int_V (\delta\varepsilon)^T \boldsymbol{\sigma}\,\mathrm{d}V = \int_V \delta\boldsymbol{u}^T \boldsymbol{f}_b\,\mathrm{d}V + \int_\Gamma \delta\boldsymbol{u}^T \boldsymbol{f}_S\,\mathrm{d}\Gamma \tag{3}$$

Received 21 August 2004; revision received 4 February 2005; accepted for publication 6 February 2005. 

*Assistant Professor, School of Mechanical Engineering, 307, Gajeon-ri, Byungcheon-myun, Cheonan-si.
†Assistant Professor, Department of Electrical and Computer Engineering, San 5 Wonchun-Dong Yeongtong-Gu.
‡Professor, School of Mechanical and Aerospace Engineering, San 56-1, Shinrim-Dong, Kwanak-Gu. Member AIAA.

$$\int_{V_p} (\delta \boldsymbol{E})^T \boldsymbol{D} \, \mathrm{d}V = \int_{\Gamma_P} q \delta\phi \, \mathrm{d}\Gamma \tag{4}$$

where $\boldsymbol{f}_s$ is surface tractions applied on the surface $\Gamma$ and is calculated from aerodynamic pressure applied to a panel, and $q$ is the electrical charge applied on the surface $\Gamma_p$ of the piezoelectric material.

### Constitutive Equations

For a lamina of the $k$th layer subject to a temperature change of $\Delta T(x, y, z)$ by aerodynamic heating under plane stress, the constitutive equations incorporating the piezoelectric effect with respect to the laminated coordinates $(x, y, z)$ are given by[3,5,8,9]

$$\boldsymbol{\sigma}^{(k)} = \begin{Bmatrix} \sigma_x \\ \sigma_y \\ \tau_{xy} \end{Bmatrix}^{(k)} = \begin{bmatrix} \bar{Q}_{11} & \bar{Q}_{12} & \bar{Q}_{16} \\ \bar{Q}_{12} & \bar{Q}_{22} & \bar{Q}_{26} \\ \bar{Q}_{16} & \bar{Q}_{26} & \bar{Q}_{66} \end{bmatrix}^{(k)} \left[ \begin{Bmatrix} \varepsilon_x \\ \varepsilon_y \\ \gamma_{xy} \end{Bmatrix} - \Delta T \begin{Bmatrix} \alpha_x \\ \alpha_y \\ \alpha_{xy} \end{Bmatrix}^{(k)} - E_3^{(k)} \begin{Bmatrix} d_x \\ d_y \\ d_{xy} \end{Bmatrix}^{(k)} \right] \tag{5}$$

where $\bar{\boldsymbol{Q}}^{(k)}$ denotes the transformed reduced stiffness matrix of the $k$th lamina, and $\alpha$ and $d$ are the transformed thermal expansion coefficients and piezoelectric strain coefficients, respectively.

### Aerodynamic Loads

First-order piston theory[1–5,8,9,19] can suitably describe the aerodynamic pressure loads acting on the panel under sufficiently high supersonic Mach number ($\sqrt{2} < M_\infty < 5$). This theory relates the aerodynamic pressure and panel transverse deflection as follows:

$$p_a = -\left( \lambda \frac{D_{110}}{a^3} \frac{\partial w}{\partial x} + \frac{g_a}{\omega_0} \frac{D_{110}}{a^4} \frac{\partial w}{\partial t} \right) \tag{6}$$

The nondimensional aerodynamic pressure parameter $\lambda$ and nondimensional aerodynamic damping $g_a$ can be defined as follows:

$$\lambda = \frac{\rho_a V_\infty^2 a^3}{\beta D_{110}}, \qquad g_a = \frac{\rho_a V_\infty \left( M_\infty^2 - 2 \right)}{\rho h \beta^3} \tag{7}$$

where the parameter $\beta$ is defined as $\beta = \sqrt{(M_\infty^2 - 1)}$, $M_\infty$ is the Mach number, $\rho_a$ is the airflow density, $V_\infty$ is the airflow velocity, $w$ is the panel transverse deflection, $D_{110}$ is the first entry of the laminate bending stiffness matrix calculated when all of the fibers of the composite layers are aligned in the direction of the airflow ($x$ direction), a reference frequency is defined by $\omega_0 = (D_{110}/\rho h a^4)^{\frac{1}{2}}$, and the nondimensional mass parameters of air-panel mass ratio and aerodynamic damping coefficient are introduced as $\mu = \rho_a a / m_{\mathrm{ave}}$, $c_a = [(M_\infty^2 - 2)/(M_\infty^2 - 1)]^2 (\mu/\beta)$.

### Kinematic Relations

The von Kármán plate model is employed for large deflection response. The von Kármán's large displacement small strains associated with displacement fields are given by

$$\boldsymbol{\varepsilon} = \begin{Bmatrix} \varepsilon_x \\ \varepsilon_y \\ \gamma_{xy} \end{Bmatrix} = \begin{Bmatrix} u^0_{,x} \\ v^0_{,y} \\ u^0_{,x} + v^0_{,y} \end{Bmatrix} + \frac{1}{2} \begin{Bmatrix} w^2_{,x} \\ w^2_{,y} \\ 2 w_{,x} w_{,y} \end{Bmatrix} + z \begin{Bmatrix} -w_{,xx} \\ -w_{,yy} \\ -2 w_{,xy} \end{Bmatrix} = \boldsymbol{\varepsilon}_m^L + \boldsymbol{\varepsilon}_m^N + z\boldsymbol{k} \tag{8}$$

where $u^0$ and $v^0$ are the midsurface in-plane displacements measured along the $x$ and $y$ coordinate axes, respectively; and $w$ is the midplane transverse bending displacement measured along the $z$ axes normal to plane of the pane.

## III. Finite Element Discretization

Spatial discretization is performed using four-node rectangular $C^1$ conforming plate elements. There are two in-plane degrees of freedom $(u^0, v^0)$ and four bending degrees of freedom $(w, w_x, w_y, w_{xy})$ at each node and one electrical degree of freedom $\phi$ per piezoelectric layer per element; that is, electric potential $\phi$ is assumed to be constant over an element piezoelectric layer and applied or detected in the center of each element piezoelectric layer.

One can obtain the global equations of motion for electromechanically integrated composite structures by assembling the element matrices for the entire system.[3,5,8]

$$\boldsymbol{M}\ddot{\boldsymbol{W}} + \boldsymbol{C}\dot{\boldsymbol{W}} + (\lambda \boldsymbol{K}_A + \boldsymbol{K}_0 - \boldsymbol{K}_{\Delta T} + \boldsymbol{K}_1 + \boldsymbol{K}_2)\boldsymbol{W} + \boldsymbol{K}_{w\phi}\boldsymbol{\varphi} = \boldsymbol{F}_{\Delta T} \tag{9}$$

$$\boldsymbol{K}_{\phi w}\boldsymbol{W} + \boldsymbol{K}_{\phi\phi}\varphi = \boldsymbol{F}_q \tag{10}$$

where $\boldsymbol{M}$ is the mass matrix; $\boldsymbol{C}$ is the aerodynamic damping matrix; $\boldsymbol{K}_A$ denotes the skew-symmetrical aerodynamic influence matrix[3,5]; $\boldsymbol{K}_{\Delta T}$ is the temperature induced geometric stiffness; $\boldsymbol{K}_A$, $\boldsymbol{K}_0$, and $\boldsymbol{K}_{\Delta T}$ are linear stiffness matrices; $\boldsymbol{K}_1$ and $\boldsymbol{K}_2$ are the first-order nonlinear stiffness and second-order nonlinear stiffness matrices, which depend linearly and quadratically on the displacements, respectively[2,3,5,8,9]; $\boldsymbol{K}_{w\phi}$ is the elastic-electric coupling stiffness matrix; $\boldsymbol{K}_{\phi\phi}$ denotes the dielectric stiffness matrix; and $\boldsymbol{F}_{\Delta T}$ and $\boldsymbol{F}_q$ are the thermal load and applied electrical charge, respectively. Substituting Eq. (10) into Eq. (9), we get

$$\boldsymbol{M}\ddot{\boldsymbol{W}} + \boldsymbol{C}\dot{\boldsymbol{W}} + \left(\lambda \boldsymbol{K}_A + \boldsymbol{K}_0 - \boldsymbol{K}_{\Delta T} + \boldsymbol{K}_1 + \boldsymbol{K}_2 - \boldsymbol{K}_{w\phi}\boldsymbol{K}_{\phi\phi}^{-1}\boldsymbol{K}_{w\phi}\right)\boldsymbol{W} = \boldsymbol{F}_{\Delta T} + \boldsymbol{K}_{w\phi}\boldsymbol{V}_a \tag{11}$$

where $\boldsymbol{V}_a$ is the actuator voltage. It might be necessary to add noise terms to represent process and measure noise in practical applications.

In the developments of the control system design and dynamic analysis, it is generally impractical to consider all modeled modes because of the large degrees of freedom of the system equations of motion. To obtain an approximate reduced-order dynamic model of the system, the mode superposition method is employed. For a simply supported rectangular panel with zero airflow angle, it is well known that the response of panel flutter produces good results even though one considers the first few modes in the airflow direction and the first mode in the spanwise direction.[3]

One can obtain the reduced nonlinear coupled-modal space form of Eq. (11) as

$$\boldsymbol{\eta}_{,\tau\tau} + \tilde{\boldsymbol{C}}\boldsymbol{\eta}_{,\tau} + (\tilde{\boldsymbol{K}} + \tilde{\boldsymbol{K}}_1 + \tilde{\boldsymbol{K}}_2)\boldsymbol{\eta} = \tilde{\boldsymbol{F}}_{\Delta T} + \tilde{\boldsymbol{K}}_{w\phi}\boldsymbol{V}_a \tag{12}$$

where $\tau = \omega_0 t$ is the nondimensional time variable.

In Eq. (12), we define $\tilde{\boldsymbol{K}}_{w\phi}$ as modal control force per unit voltage. The modal displacement $\boldsymbol{\eta}$ can be calculated by using any numerical integration scheme such as the Newmark-$\beta$ or Runge–Kutta method.

## IV. Nonlinear Feedback Linearization Control Law

### State Equation

The design of active control system is carried out in state-space form. Introducing the state-space variable $\boldsymbol{E} = [\boldsymbol{\eta} \ \ \boldsymbol{\eta}_{,\tau}]^T \in \boldsymbol{R}^{12 \times 1}$, the second-order nonlinear coupled-modal equation given by Eq. (12) can be converted to a first-order state-space model as

$$\dot{\boldsymbol{E}} = \boldsymbol{A}\boldsymbol{E} + \boldsymbol{B}\boldsymbol{V}_a + \boldsymbol{Z} \tag{13}$$

where $\boldsymbol{A} \in \boldsymbol{R}^{12 \times 12}$ is the system matrix, $\boldsymbol{B} \in \boldsymbol{R}^{12 \times 1}$ is the control influence coefficient matrix, and $\boldsymbol{Z} \in \boldsymbol{R}^{12 \times 1}$ is the mechanical load matrix, which are given by

$$\boldsymbol{A} = \begin{bmatrix} 0_{6 \times 6} & \boldsymbol{I}_{6 \times 6} \\ -(\tilde{\boldsymbol{K}} + \tilde{\boldsymbol{K}}_1 + \tilde{\boldsymbol{K}}_2) & -\tilde{\boldsymbol{C}} \end{bmatrix}, \qquad \boldsymbol{B} = \begin{bmatrix} 0_{6 \times 1} \\ \tilde{\boldsymbol{K}}_{w\phi} \end{bmatrix}$$

$$\boldsymbol{Z} = \begin{bmatrix} 0_{6 \times 1} \\ \tilde{\boldsymbol{F}}_{\Delta T} \end{bmatrix} \tag{14}$$

### Feedback Linearization

In this Note, we assume that $\boldsymbol{A}$, $\boldsymbol{B}$, and $\boldsymbol{Z}$ in Eq. (14) are available. Then, we can apply the feedback linearization control method.[10] Because the number of the state variables to be controlled in the system (13) ($\boldsymbol{\eta} \in \boldsymbol{R}^{6\times 1}$) is larger than that of the available control input ($\boldsymbol{V}_a \in \boldsymbol{R}^1$), the system (13) is an underactuated system. Accordingly, we need to use the pseudoinverse $\tilde{\boldsymbol{K}}^{+}_{w\phi}$, instead of inverse $\tilde{\boldsymbol{K}}^{-1}_{w\phi}$.

Thus, we employ the control law

$$\boldsymbol{V}_a = \tilde{\boldsymbol{K}}^{+}_{w\varphi}\{-\tilde{\boldsymbol{F}}_{\Delta T} + \boldsymbol{u}\} \tag{15}$$

where $\tilde{\boldsymbol{K}}^{+}_{w\phi} = (\tilde{\boldsymbol{K}}^{T}_{w\phi}\tilde{\boldsymbol{K}}_{w\phi})^{-1}\tilde{\boldsymbol{K}}^{T}_{w\phi}$ and $\boldsymbol{u} \in \boldsymbol{R}^{6\times 1}$. Then, Eq. (13) becomes

$$\begin{aligned}\dot{\boldsymbol{E}} &= \boldsymbol{A}\boldsymbol{E} + \begin{bmatrix} 0_{6\times 1} \\ \tilde{\boldsymbol{F}}_{\Delta T} + \tilde{\boldsymbol{K}}_{w\phi}\tilde{\boldsymbol{K}}^{+}_{w\varphi}\{-\tilde{\boldsymbol{F}}_{\Delta T} + \boldsymbol{u}\}\end{bmatrix} \\ &= \boldsymbol{A}\boldsymbol{E} + \begin{bmatrix} 0_{6\times 1} \\ \boldsymbol{u}\end{bmatrix} + \begin{bmatrix} 0_{6\times 1} \\ \left(-\boldsymbol{I}_{6\times 6} + \tilde{\boldsymbol{K}}_{w\phi}\tilde{\boldsymbol{K}}^{+}_{w\varphi}\right)\{-\tilde{\boldsymbol{F}}_{\Delta T} + \boldsymbol{u}\}\end{bmatrix}\end{aligned} \tag{16}$$

Note that the last term of the right-hand side in Eq. (16) remains because the controlled system is underactuated and $\tilde{\boldsymbol{K}}^{+}_{w\phi}$ is used in Eq. (15). Because $\boldsymbol{A}$ is not Hurwitz, $\boldsymbol{u}$ is designed to cancel the nonlinear terms of $\boldsymbol{A}$ in Eq. (14) as

$$\boldsymbol{u} = (\tilde{\boldsymbol{K}} + \tilde{\boldsymbol{K}}^1 + \tilde{\boldsymbol{K}}^2)\boldsymbol{\eta} + \tilde{\boldsymbol{C}}\boldsymbol{\eta}_{,\tau} + \boldsymbol{v} \tag{17}$$

where $\boldsymbol{v}$ is additional control input to be designed later in Eq. (20). Also, Eq. (16) becomes

$$\dot{\boldsymbol{E}} = \boldsymbol{A}_0\boldsymbol{E} + \begin{bmatrix} 0_{6\times 1} \\ \boldsymbol{v}\end{bmatrix} + \begin{bmatrix} 0_{6\times 1} \\ \left(-\boldsymbol{I}_{6\times 6} + \tilde{\boldsymbol{K}}_{w\phi}\tilde{\boldsymbol{K}}^{+}_{w\varphi}\right)\{-\tilde{\boldsymbol{F}}_{\Delta T} + \boldsymbol{u}\}\end{bmatrix} \tag{18}$$

where

$$\boldsymbol{A}_0 = \begin{bmatrix} 0_{6\times 6} & \boldsymbol{I}_{6\times 6} \\ 0_{6\times 6} & 0_{6\times 6}\end{bmatrix} \tag{19}$$

Finally, if $\boldsymbol{v}$ is chosen as

$$\boldsymbol{v} = -\boldsymbol{A}_m\boldsymbol{\eta}_{,\tau} - \boldsymbol{B}_m\boldsymbol{\eta} \tag{20}$$

where $\boldsymbol{A}_m = \mathrm{diag}(a_{m1}, \ldots, a_{m6}) \in \boldsymbol{R}^{6\times 6}$ and $\boldsymbol{B}_m = \mathrm{diag}(b_{m1}, \ldots, b_{m6}) \in \boldsymbol{R}^{6\times 6}$ are positive-definite matrices, then Eq. (18) can be changed into

$$\dot{\boldsymbol{E}} = \boldsymbol{A}_s\boldsymbol{E} + \begin{bmatrix} 0_{6\times 1} \\ \left(-\boldsymbol{I}_{6\times 6} + \tilde{\boldsymbol{K}}_{w\phi}\tilde{\boldsymbol{K}}^{+}_{w\varphi}\right)\{-\tilde{\boldsymbol{F}}_{\Delta T} + \boldsymbol{u}\}\end{bmatrix} \tag{21}$$

where

$$\boldsymbol{A}_s = \begin{bmatrix} 0_{6\times 6} & \boldsymbol{I}_{6\times 6} \\ -\boldsymbol{B}_m & -\boldsymbol{A}_m\end{bmatrix} \tag{22}$$

Here, design parameters $a_{\mathrm{mi}}$ and $b_{\mathrm{mi}}$ in $\boldsymbol{A}_m$ and $\boldsymbol{B}_m$ for $i = 1, \ldots, 6$ are chosen as $a_{\mathrm{mi}} = 2\zeta_i\omega_{\mathrm{ni}}$ and $b_{\mathrm{mi}} = \omega^2_{\mathrm{ni}}$.

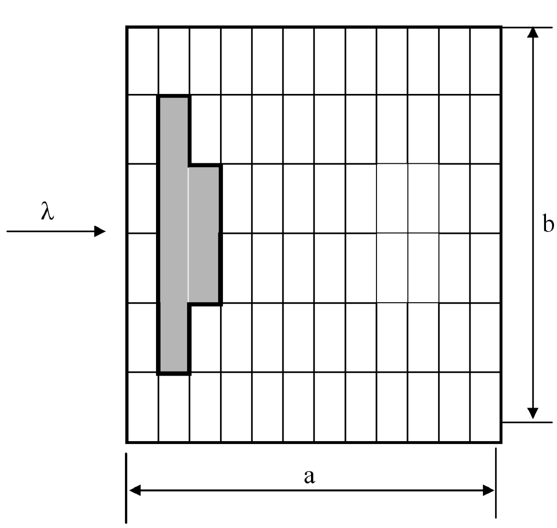


**Fig. 1 Placement of PZT actuator on composite plate.**

## V. Numerical Results

The simply supported symmetrically laminated eight-layer [45 deg/−45 deg/90 deg/0 deg]$_s$ square graphite/epoxy composite plate[9] is used for the numerical simulations. The in-plane displacements at the edges are considered to be immovable. The dimensions of the composite plate are 0.3 × 0.3 × 0.001 m, and the plate is discretized using the $C^1$ conforming four-node rectangular element with 12 elements in the $x$ direction (flow direction) and six elements in the $y$ direction as shown in Fig. 1. The PZT material is used as an actuator and is bonded on the top and bottom surfaces of the panel. The piezoelectric layer thickness is selected

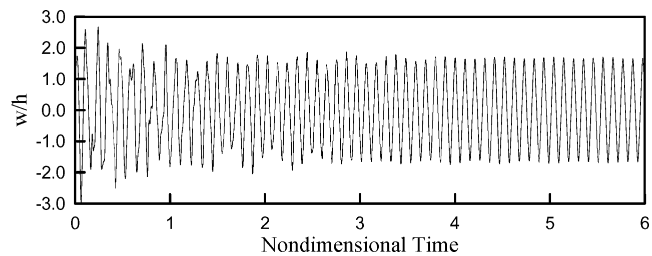


**Fig. 2 Time history of a simply supported composite panel at $\Delta T/\Delta T_{\mathrm{cr}} = 0$ and $\lambda = 900$.**

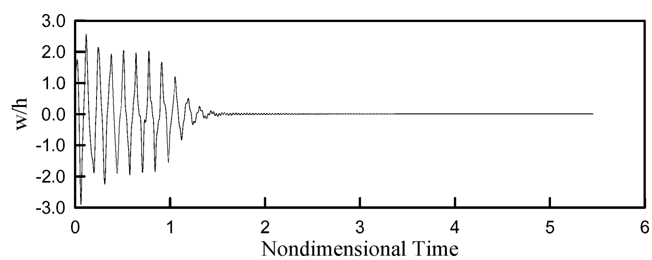


**a) Time history of panel motion with LQR based on the linear model**

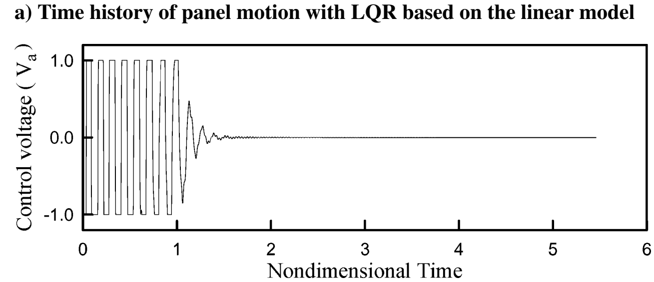


**b) Control input with LQR based on the linear model**

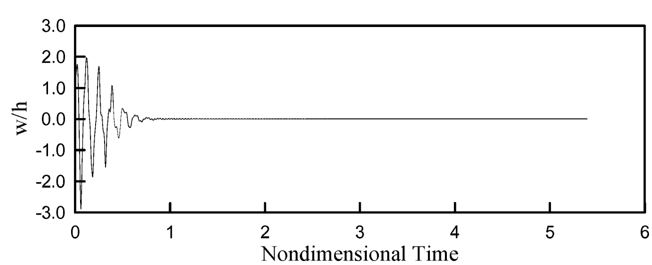


**c) Time history of panel motion with feedback linearization control**

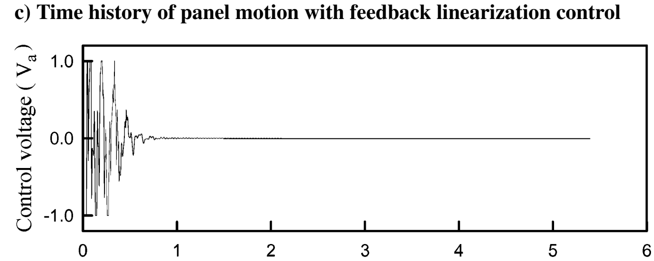


**d) Control input with feedback linearization control**

**Fig. 3 Time history of panel motion and control input with controller at $\lambda = 900$.**

to be 0.0005 m. The aerodynamic damping coefficient[2,3,5] $C^a$ is taken to be 0.01, and temperature distribution is assumed to be $\Delta T = T_0 \sin(\pi x/a) \sin(\pi y/b)$. The responses of the panel motion are observed at a maximum deflection location with coordinates $x = 0.75a$ and $y = 0.5b^3$ using Newmark-$\beta$ time-integration scheme.

Figure 1 shows the shape and location of the piezoceramic patches. According to Refs. 5 and 20, to locate piezoelectric actuators in the vicinity of leading edge gives rise to the higher critical dynamic pressure and $\lambda_{\max}$. The critical buckling temperature is calculated to be 18.37°C for the panel with the piezoelectric actuators shown in Fig. 1. The flutter suppression results by the feedback linearization controller based on the nonlinear model are compared with suppression results by a LQR[5,8] based on the linear model. Design parameters of $a_{\mathrm{mi}} = 2\zeta\omega_{\mathrm{ni}}$ in Eq. (20) are chosen as $\zeta_i = 0.707$. The piezolaminated composite panel at the dynamic pressure $\lambda = 900$ exhibits limit-cycle motions as shown in Fig. 2. Time history of flutter motions and control input with a LQR based on the linear model and feedback linearization controller based on the nonlinear model are shown in Fig. 3. As shown in the figure, the limit-cycle motions are completely suppressed by both controllers. But, the saturation is more likely to happen in the case of LQR controller because the previous LQR controller is based on the linear model, compared to the proposed nonlinear controller. Feedback linearization controller based on the nonlinear model effectively suppresses the flutter motions with a lower control input.

## VI. Conclusions

The nonlinear characteristics of the modal equations are fully considered in the design of the nonlinear controller. Through simulation results, we could observe that the proposed controller can effectively suppress the flutter. We can expect that similar results of aircraft wing can be obtained for the structures with similar shapes. Because the actual system has uncertainties inevitably and this causes performance degradation, we need to compensate for these uncertainties in system dynamics by using adaptive and robust control methods in the future work. Also, because all states might not be available in actual situation, nonlinear observer design can be useful as a practical further study.

## Acknowledgment

This work was supported by Korea Research Foundation Grant (KRF-2004-003-D00068).

## References

[1]Gray, C. E., Jr., and Mei, C., "Large Amplitude Finite Element Flutter Analysis of Composite Panels in Hypersonic Flow," *AIAA Journal*, Vol. 31, No. 6, 1993, pp. 1090–1099.

[2]Mei, C., Abedl-Motagaly, K., and Chen, R., "Review of Nonlinear Panel Flutter at Supersonic and Hypersonic Speeds," *Applied Mechanics Reviews*, Vol. 52, No. 10, 1999, pp. 321–332.

[3]Zhou, R. C., Xue, D. Y., and Mei, C., "A Finite Element Time Domain-Modal Formulation for Nonlinear Flutter of Composite Panels," *AIAA Journal*, Vol. 32, No. 10, 1994, pp. 2044–2052.

[4]Scott, R. C., and Weisshaar, T. A., "Controlling Panel Flutter Using Adaptive Materials," AIAA Paper 91-1067, 1991; also *Journal of Aircraft*, Vol. 31, No. 1, 1994, pp. 213–222.

[5]Zhou, R. C., Lai, Z., Xue, D. Y., Hauang, J.-K., and Mei, C., "Suppression of Nonlinear Panel Flutter with Piezoelectric Actuators Using Finite Element," *AIAA Journal*, Vol. 33, No. 6, 1995, pp. 1098–1105.

[6]Frampton, K. D., Clark, R. L., and Dowell, E. H., "Active Control of Panel Flutter with Linearized Potential Flow Aerodynamics," AIAA Paper 95-1079, Feb. 1995.

[7]Suleman, R., and Goncalves, M. A., "Optimization Issues in Applications of Piezoelectric Actuators in Panel Flutter Controls," *Proceedings of SPIE-International Society for Optical Engineering*, Society of Photo-Optical Instrumentation Engineers (International Society for Optical Engineering), edited by V. V. Varadan and J. Chandra, Vol. 3049, 1997, pp. 335–347.

[8]Moon, S. H., and Kim, S. J., "Active and Passive Suppressions of Nonlinear Panel Flutter Using Finite Element Method," *AIAA Journal*, Vol. 11, No. 11, 2001, pp. 2042–2050.

[9]Moon, S. H., and Kim, S. J., "Suppression of Nonlinear Composite Panel Flutter with Active/Passive Hybrid Piezoelectric Networks Using Finite Element Method," *Composite Structures*, Vol. 59, No. 4, 2003, pp. 525–533.

[10]Slotine, J.-J. E., and Li, W., *Applied Nonlinear Control*, Prentice–Hall, 1991.

[11]Spong, M. W., and Vidyasagar, M., *Robot Dynamics and Control*, Wiley, New York, 1989.

[12]Chwa, D., and Choi, J. Y., "New Parametric Affine Modeling and Control for Skid-to-Turn Missiles," *IEEE Transactions on Control Systems Technology*, Vol. 9, No. 2, 2001, pp. 335–347.

[13]Dawson, D. M., Hu, J., and Burg, T. C., *Nonlinear Control of Electric Machinery*, Marcel Dekker, New York, 1998.

[14]Kolmanovsky, I., and McClamroch, N. H., "Developments in Non-Holonomic Control Problems," *IEEE Control Systems*, Vol. 15, No. 6, 1995, pp. 20–36.

[15]Lee, T-. C., Song, K-. T., Lee, C-. H., and Teng, C-. C., "Tracking Control of Unicycle-Modeled Mobile Robots Using a Saturation Feedback Controller," *IEEE Transactions on Control Systems Technology*, Vol. 9, No. 2, 2001, pp. 305–318.

[16]Coron, J. -M., and Kerai, E. -Y., "Explicit Feedbacks Stabilizing the Attitude of a Rigid Spacecraft with Two Control Torques," *Automatica*, Vol. 32, No. 5, 1996, pp. 669–677.

[17]Reyhanoglu, M., "Exponential Stabilization of an Underactuated Autonomous Surface Vessel," *Automatica*, Vol. 33, No. 12, 1997, pp. 2249–2254.

[18]Kermani, M. R., Moallem, M., and Patel, R. V., "Parameter Selection and Control Design for Vibration Suppression Using Piezoelectric Transducers," *Control Engineering Practice*, Vol. 12, No. 8, 2004, pp. 1005–1015.

[19]Bisplinghoff, R. L., and Ashley, H., *Principles of Aeroelasticity*, Wiley, New York, 1962.

[20]Ho, M. T., Chen, R., and Chu, L. C., "Wind-Tunnel Testing of Panel Flutter Control Using Piezoelectric Actuation and Iterative Gain Tuning," *SPIE Conference Smart Structures and Materials*, Society of Photo-Optical Instrumentation Engineers (International Society for Optical Engineering), edited by M. E. Regelbrugge, Vol. 3041, 1997, pp. 564–577.

M. Ahmadian
*Associate Editor*